

Optimization of thermoelectric properties in elemental tellurium via high pressure

Dongyao Zhao(赵东尧), Manman Yang(杨曼曼), Hairui Sun(孙海瑞), Xin Chen(陈欣), Yongsheng Zhang(张永胜), and Xiaobing Liu(刘晓兵)

Citation: Chin. Phys. B, 2023, 32 (**10**): 107305. DOI: 10.1088/1674-1056/ace15e
Journal homepage: http://cpb.iphy.ac.cn; http://iopscience.iop.org/cpb

What follows is a list of articles you may be interested in

Strong anharmonicity-assisted low lattice thermal conductivities and high thermoelectric performance in double-anion Mo_2AB_2(A=S, Se, Te; B=Cl, Br, I) semiconductors

Haijun Liao(廖海俊) Le Huang(黄乐), Xing Xie(谢兴), Huafeng Dong(董华锋), Fugen Wu(吴福根) Zhipeng Sun(孙志鹏), and Jingbo Li(李京波)
Chin. Phys. B, 2023, 32 (**10**): 107304. DOI: 10.1088/1674-1056/ace314

Thermoelectric generators and their applications: Progress, challenges, and future prospects

Nassima Radouane
Chin. Phys. B, 2023, 32 (**5**): 057307. DOI: 10.1088/1674-1056/aca5fd

Thermoelectric signature of Majorana zero modes in a T-typed double-quantum-dot structure

Cong Wang(王聪) and Xiao-Qi Wang(王晓琦)
Chin. Phys. B, 2023, 32 (**3**): 037304. DOI: 10.1088/1674-1056/ac92d3

Research status and performance optimization of medium-temperature thermoelectric material SnTe

Pan-Pan Peng(彭盼盼), Chao Wang(王超), Lan-Wei Li(李岚伟), Shu-Yao Li(李淑瑶), and Yan-Qun Chen(陈艳群)
Chin. Phys. B, 2022, 31 (**4**): 047307. DOI: 10.1088/1674-1056/ac20c9

Pressure-mediated contact quality improvement between monolayer MoS_2 and graphite

Mengzhou Liao(廖梦舟), Luojun Du(杜罗军), Tingting Zhang(张婷婷), Lin Gu(谷林), Yugui Yao(姚裕贵), Rong Yang(杨蓉), Dongxia Shi(时东霞), Guangyu Zhang(张广宇)
Chin. Phys. B, 2019, 28 (**1**): 017301. DOI: 10.1088/1674-1056/28/1/017301

Optimization of thermoelectric properties in elemental tellurium via high pressure

Dongyao Zhao(赵东尧)[1,†], Manman Yang(杨曼曼)[1,†], Hairui Sun(孙海瑞)[1,2,‡], Xin Chen(陈欣)[1,2], Yongsheng Zhang(张永胜)[1,2], and Xiaobing Liu(刘晓兵)[1,2,§]

[1] *Laboratory of High-Pressure Physics and Materials Science (HPPMS), School of Physics and Physical Engineering, Qufu Normal University, Qufu* 273165, *China*

[2] *Advanced Research Institute of Multidisciplinary Sciences, Qufu Normal University, Qufu* 273165, *China*

(Received 21 April 2023; revised manuscript received 9 June 2023; accepted manuscript online 25 June 2023)

High pressure and high temperature (HPHT) technology, as an extreme physical condition, plays an important role in regulating the properties of materials, having the advantages of enhancing doping efficiency, refining grain size, and manufacturing defects, therefore it is quite necessary to study the effectiveness on tuning thermoelectric properties. Elemental telluride, a potential candidate for thermoelectric materials, has the poor doping efficiency and high resistivity, which become an obstacle for practical applications. Here, we report the realization of a dual optimization of electrical behaviors and thermal conductivity through HPHT method combining with the introduction of black phosphorus. The results show the maximum zT of 0.65 and an average zT of 0.42 (300 K–610 K), which are increased by 55% and 68% in the synthesis pressure regulation system, respectively. This study clarifies that the HPHT method has significant advantages in modulating the thermoelectric parameters, providing a reference for seeking high performance thermoelectric materials.

Keywords: high pressure, thermoelectric, thermal conductivity, power factor

PACS: 73.50.Lw, 91.60.Gf, 61.82.Fk **DOI:** 10.1088/1674-1056/ace15e

With the advent of the electronic information age, it has become the strategic focus of sustainable development to build a new energy system, develop green and recyclable renewable resources and improve energy conversion efficiency.[1,2] Thermoelectric materials with the most potential candidate for environmental energy are mainly determined by the dimensionless coefficient $zT = S^2T/\rho(\kappa_e + \kappa_{ph} + \kappa_{bip})$, where S is Seebeck coefficient, ρ is resistivity, T is Kelvin temperature, κ_e, κ_{ph}, and κ_{bip} are electron, phonon, and bipolar thermal conductivities, respectively.[3–5] However, due to the strong coupling between carriers and phonons, it is a great challenge to optimize the related parameters together. Over the past few decades, classical, high-performance, multicomponent compounds such as Bi_2Te_3 and SnSe have produced encouraging results.[6–10] However, the diversity of elements leading to the segregation and complex structure increases the difficulty to get clear about the mechanism of the improvement. Hence, many research have been focused on single-element semiconductors.[11,12]

Elemental semiconductor thermoelectric materials, such as black phosphorus (BP) and tellurium (Te), provide a better basis for interpreting the relationship between the internal physical parameters of the material due to the unicity of the elements. Theoretical predictions demonstrate that BP and its derivatives show great potential for novel eco-friendly thermoelectric applications because of the unique in-plane anisotropic electronic structure.[10,13–19] Element Te, a narrow band gap semiconductor, has been considered as a potential candidate for thermoelectric materials because of its high degeneracy, large effective mass and high Seebeck coefficient.[20] Many attempts have been made to further improve the efficiency of thermoelectric conversion.[21,22] Lin *et al.* realized doping by hot pressing, and finally optimize the carrier concentration to 2.65×10^{19} cm^{-3}, thus improving the electrical properties of Te.[23] An *et al.* used the spark plasma sintering (SPS) method combined with the intrinsic quasi-one-dimensional (1D) structure of the sample, which contributed to form the chain texture along the crystallographic *c*-axial direction, to optimize the carrier and phonon scattering to a certain extent.[24] Su *et al.* effectively replaced the alloying of samples by using the high pressure and high temperature (HPHT) method, and the phonon thermal conductivity of the material decreased from 0.65 W·m^{-1}·K^{-1} to 0.45 W·m^{-1}·K^{-1}, which optimized the phonon transport and ultimately improved the thermoelectric performance.[25] Therefore, it is not hard to see that an effective synthesis method is vital to obtain high quality thermoelectrics. Among them, HPHT technology is playing an important role in synthesizing specimens because of the

[†]These authors contributed equally to this work.

[‡]Corresponding author. E-mail: hairuisun1216@qfnu.edu.cn

[§]Corresponding author. E-mail: xiaobing.phy@qfnu.edu.cn

© 2023 Chinese Physical Society and IOP Publishing Ltd

advantages, such as time-saving, high efficiency, manufacturing defects and controllable reaction conditions.[25–29] In our previous work, we constructed a BP-Te heterogeneous structure to optimize the thermoelectric performance of Te through HPHT method.[16] Hence, it is essential to investigate the effect of pressure on Te.

In this work, we successfully synthesized Te samples with doping BP under different pressures to explore the impact of pressure on electrical and thermal properties. Our results demonstrate that zT vlues of Te-based materials are greatly improved under high pressure. The maximum zT value (zT_{max}) and the average zT value (zT_{ave}) of Te + 0.25 wt% GeP_5 samples synthesized at 5.5 GPa are significantly enhanced by 55% (68%) compared to 3.0 GPa. Moreover, with the content of GeP_5 increasing, the performance is further optimized. Thus, high pressure is proved to be an effective means for seeking high performance thermoelectrics.

Using high purity germanium (Ge, 99.999%) and phosphorus (P, 99.999%) ingot as raw material, single crystal GeP_5 was prepared by HPHT method. The high purity Te ingot (99.999%) and GeP_5 were weighed by mass ratio. The raw materials were then packaged in a mortar and ground for an hour. Then the target polycrystalline samples were prepared at 1000 K and 3.0 GPa–5.5 GPa for 30 minutes through HPHT method.

The crystal structures of powder samples had been characterized by Cu-$K\alpha$ radiation x-ray diffraction (XRD) (PANalytical X'pert3, Holland). Raman spectroscopy (HR Evolution, JY Horiba) was carried on a spectrometer with excitation wavelength of 633 nm. The surface morphology and element distribution of the samples were tested by scanning electron microscope (SEM, Carl Zeiss Sigma 500 VP). TEM images were obtained on a Thermo Fisher Talos F200S G2 (United States). The carrier-dependent parameters were measured at room temperature on the Hall device (Lake Shore 8404, USA) using van der Pauw geometry. Resistivity (ρ) and Seebeck coefficient (S) were measured simultaneously in CTA-3s (Cryoall China). Thermal conductivity (κ) is calculated by $\kappa = D \times C_p \times d$ where D is the thermal diffusion coefficient measured on a laser heat-conducting instrument (Netzsch LFA457, Germany). The heat capacity (C_p) values were estimated by Dulong–Petit law. The density (d) was determined by Archimedean principle.

Figure 1(a) shows powder x-ray diffraction (XRD) data of Te and GeP_5-composited Te samples synthesized under different pressures. The collected XRD patterns can be well characterized as hexagonal structure of $P3_121$ group.[30] As shown in the figure, no other second phase was observed. Figure 1(b) shows the typical Raman spectra of all sample prepared under various pressures. It can be observed that the peaks located at 91 cm^{-1}, 119 cm^{-1}, 138 cm^{-1} are correspond to the three characteristic peaks of elemental Te phase, representing the three vibration modes E^1, A_1, and E^2, respectively.[31] Meanwhile, three obvious characteristic peaks at 358 cm^{-1}, 434 cm^{-1}, and 462 cm^{-1}, can be attributed to BP phase, representing A_g^1, B_{2g}, and A_g^2 vibration modes, respectively.[32] The results show that GeP_5 decomposed into BP and Ge via HPHT conditions.

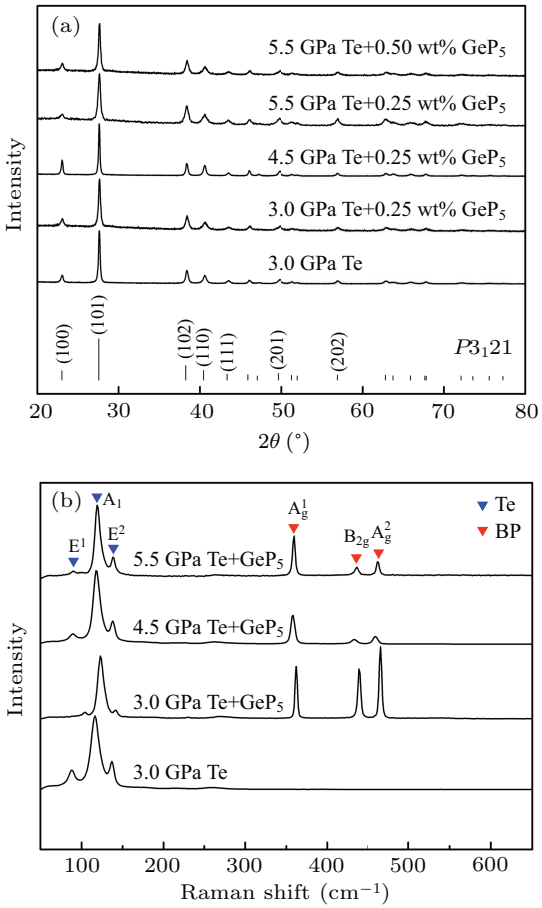


Fig. 1. Phase characterization of produced GeP_5-composited Te samples under different synthetic pressures: (a) XRD patterns and (b) Raman spectrum.

Hall effect test of the prepared samples was carried out at room temperature, listed in Table 1. The positive Hall coefficient reveal that all samples are p-type semiconductor. It can be seen that the introduction of GeP_5 significantly increased the carrier concentration (n_H) of Te. The decomposed Ge has two less electron than Te, and when it replaces Te as an acceptor impurity, it can introduce holes, meaning that the electrons in the valence band are transferred to the acceptor level, which leads to a significant increase in hole concentration. More importantly, with the synthetic pressure increasing, we find that the n_H are improved up to 2.5 $\times 10^{19}$ cm^{-3}, which is two orders of magnitude higher than the pure Te sample, while the fluctuation of mobility (μ_H) is in a small range. The result leads to substantial optimization of electrical properties.

Table 1. The Hall effect test for the samples synthesized under different pressures.

Samples	Hall coefficient R_H ($cm^3 \cdot C^{-1}$)	Carrier concentration n_H (cm^{-3})	Hall mobility μ_H ($cm^2 \cdot V^{-1} \cdot s^{-1}$)
Te (3.0 GPa)	8.02	7.8×10^{17}	146.00
Te + 0.25 wt% GeP_5 (3.0 GPa)	0.31	1.9×10^{19}	95.58
Te + 0.25 wt% GeP_5 (4.5 GPa)	0.28	2.2×10^{19}	93.91
Te + 0.25 wt% GeP_5 (5.5 GPa)	0.25	2.5×10^{19}	92.62
Te + 0.50 wt% GeP_5 (5.5 GPa)	0.16	3.9×10^{19}	72.67

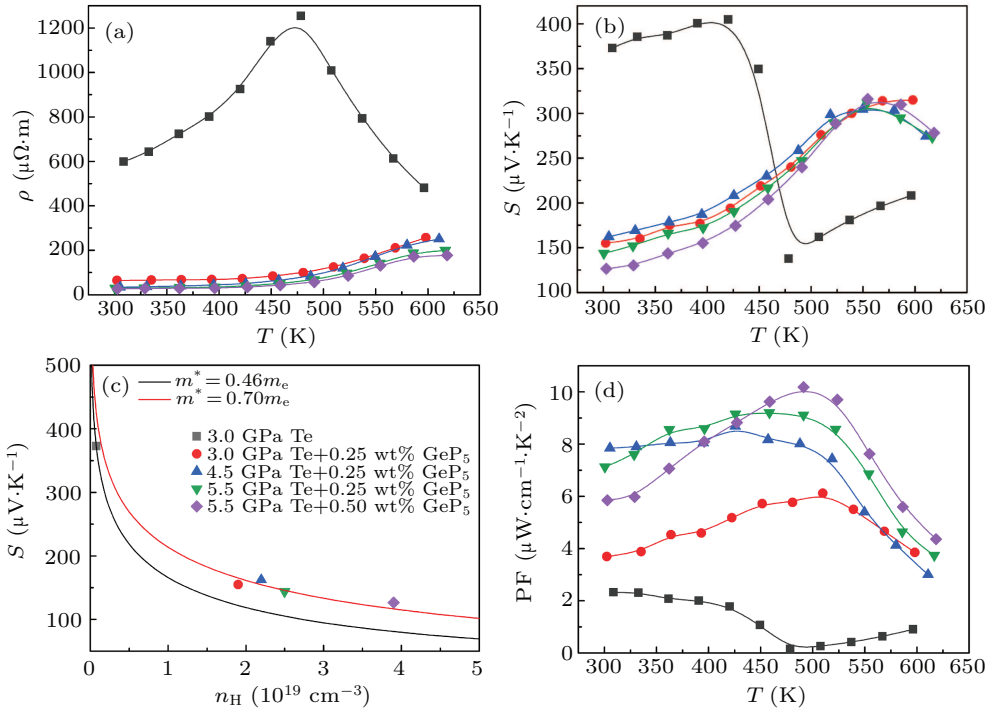


Fig. 2. Temperature-dependent electronic transport properties of Te, GeP_5-composited Te samples synthesized under different pressures. (a) Resistivity. (b) Seebeck coefficient. (c) Relationship between the carrier concentration and Seebeck coefficient. (d) Power factor (PF).

The electrical transport performance depending on temperature was measured in the range of 300 K–610 K. Figure 2(a) shows the lower resistivity of the GeP_5-composited Te samples. In addition, as plotted in Fig. 2(b), GeP_5-introduced samples exhibit higher Seebeck coefficient comparing with pristine Te when the test temperature is above 450 K. Both the parameters are optimized in higher temperature range, and the values increase continuously with the temperature increasing. When the temperature exceeds 550 K, the S gradually decreases due to the appearance of intrinsic excitation, resulting in an increase in minority carriers,[33] which restrains the S of the sample. Comparing with pure Te, the introduction of GeP_5 makes the bipolar effect move to high temperature region. Figure 2(c) shows the relationship between S and n_H based on the single parabolic band model. We can find that the carrier effective mass (m^*, black line) of pure Te is smaller than the GeP_5-composited Te samples, which can partly eliminate the reduction of S by the increasing of n_H. Combined with the changes in the ρ and S, we noted that the PF values of the sample were significantly enhanced with the synthetic pressure rising, reaching a maximum value of 10.18 $\mu W \cdot cm^{-1} \cdot K^{-2}$ at 490 K of Te + 0.50 wt% GeP_5 sample synthesized at 5.5 GPa, as shown in Fig. 2(d). Higher fabricating pressure improves the decomposition efficiency of GeP_5, thus leading to the increase of n_H, ultimately optimizing the electrical transport property.

Figures 3(a)–3(c) is the scanning electron microscope (SEM) images of the GeP_5-composited Te sample synthesized at 3.0 GPa, 4.5 GPa, and 5.5 GPa, respectively. The images show that with the increase of synthetic pressure, the grain boundaries become more abundant (as shown in Figs. 3(d)–3(e)), indicating that high pressure has an inhibitory effect on grain growth. The affluent boundaries in the sample can enhance the phonons scattering, and then reduce the phonon conductivity.[34]

Figures 4(a)–4(e) show the SEM images and the corresponding energy dispersive spectrometer (EDS) mapping of the sample synthesized at 5.5 GPa. It can be clearly observed that the BP embedded in the matrix, indicating that GeP_5 have

decomposed into Ge and P, and the elemental P has been converted into BP phase basing on the Raman results in Fig. 1(b), randomly distributing around the grain boundaries. In addition, the element Ge uniformly disperses in the basis materials, which has positive influence on the diminution of thermal conductivity.

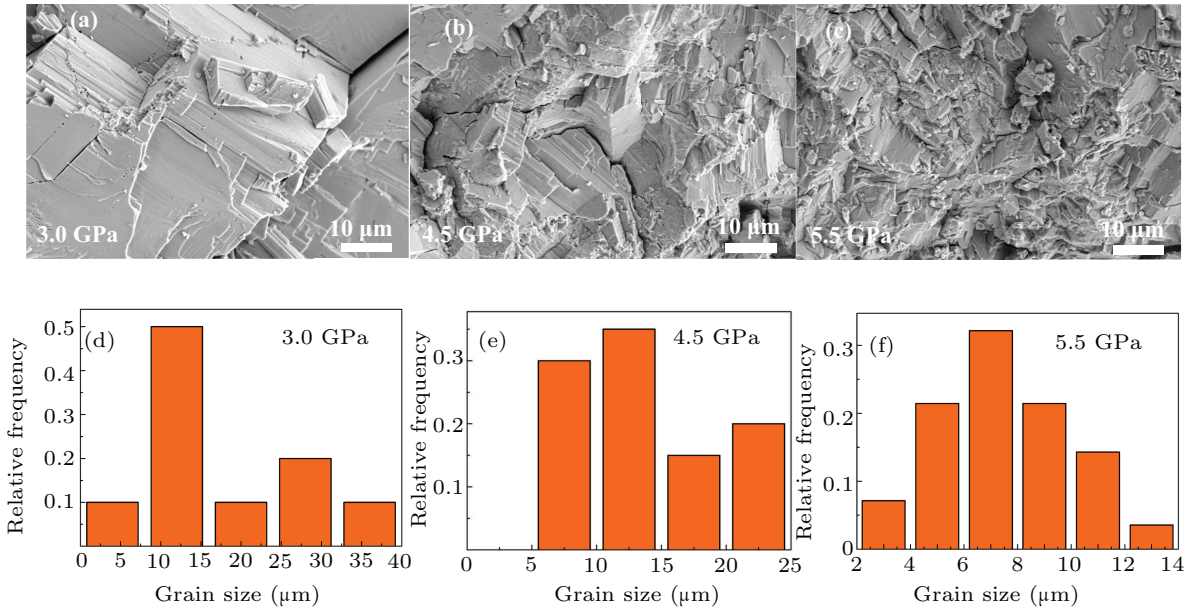


Fig. 3. (a)–(c) SEM images for the produced GeP_5-composited Te samples synthesized under different pressures, (d)–(f) grain size distribution corresponding to panels (a)–(c).

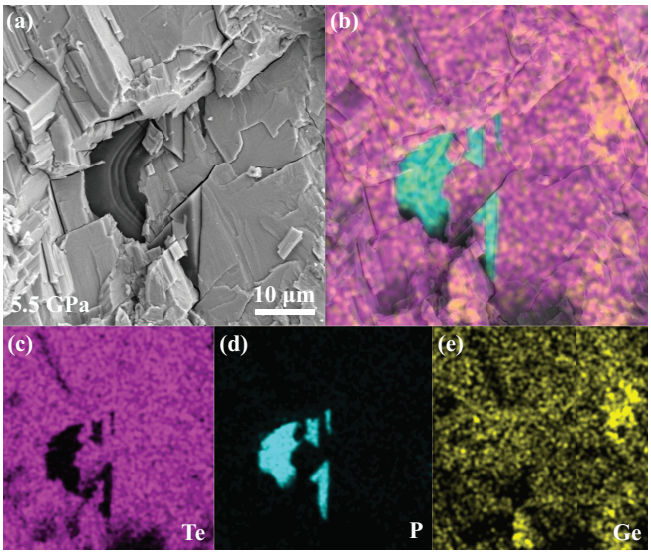


Fig. 4. (a) SEM image of Te + 0.5 wt% GeP_5, (b)–(e) the corresponding EDS elemental mappings.

The detailed microstructure of Te + 0.50 wt% GeP_5 synthesized at 5.5 GPa was characterized by high-resolution transmission electron microscopy (HRTEM) and inverse fast Fourier transform (IFFT) as shown in Fig. 5. We can observe the clear lattice fringes of the sample, and then select the yellow and red regions for IFFT in Fig. 5(a). As shown in Figs. 5(b) and 5(c), the Te can be observed in the sample, evidenced by the gauged interplanar distances of 0.323 nm, corresponding to the (101) planes. Meanwhile, (041) planes of BP is also observed, proved by the measured interplanar distances is 0.223 nm. It indicates that BP acts as the second phase in Te matrix, which is benefit for enhancing the scattering of intermediate frequency phonon. Moreover, the lattice deformation and dislocation can also be found in the domains within our samples, which can effectively disperse the transportation of phonons, reducing the lattice thermal conductivity, thus optimizing the thermoelectric properties.

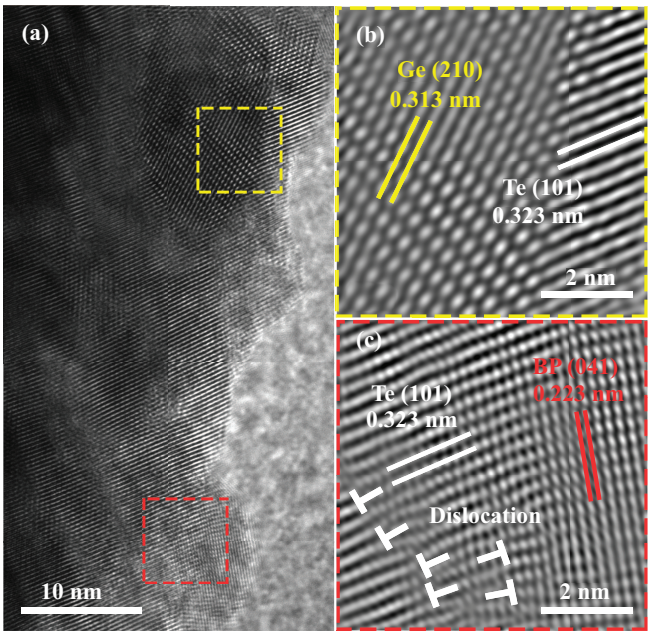


Fig. 5. Microstructure of produced GeP_5-composited Te sample: (a) HRTEM image, and (b), (c) the IFFT images.

Figure 6(a) shows the temperature dependence of the total thermal conductivity (κ) in the range of 300 K–610 K. The κ of all samples prepared under high pressure markedly de-

creases comparing with the pristine Te. With the increase of temperature, the κ gradually decreases in the range of 300 K–550 K, and then shows an upward trend due to the emergence of intrinsic excitation. The minimum thermal conductivity is achieved 0.61 $W{\cdot}m^{-1}{\cdot}K^{-1}$ at 550 K for the sample of Te + 0.25 wt% GeP_5 synthesized at 4.5 GPa. We further calculated the phonon and bipolar thermal conductivity according to Wiedemann–Franz law: $\kappa_{ph+bip} = \kappa - \kappa_e$, ($\kappa_e = L\sigma T$, L is the Lorenz number, which is estimated by the equation $L = 1.5 + \exp(-|S|/116)$,[35,36] as shown in Fig. 6(b), about 36% decrease for the sample synthesized at high pressure. The reduction of κ_{ph+bip} can be attributed to the combining effect of the existence of BP, lattice defects, and more grain boundary density introduced by high pressure.

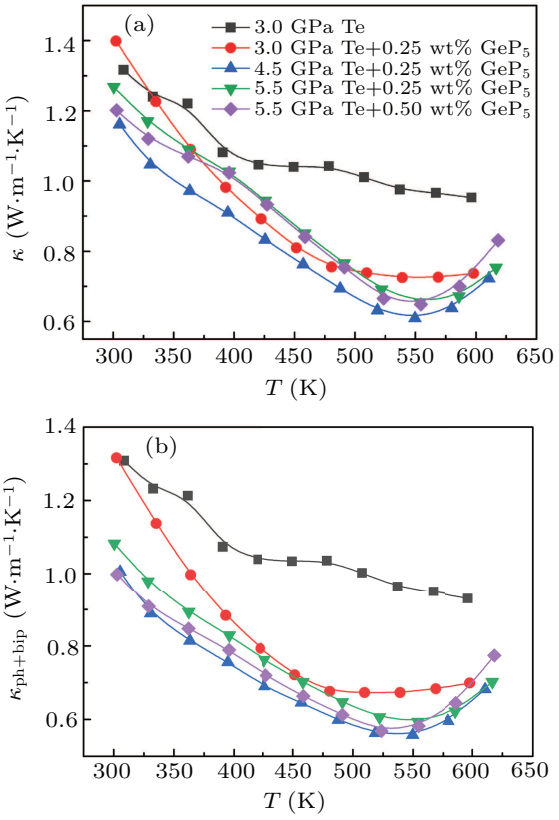


Fig. 6. Temperature-dependent of Te, GeP_5-composited Te samples under different synthetic pressures: (a) total thermal conductivity and (b) phonon and bipolar thermal conductivities.

Benefitting from the superiority of high pressure and the introduction of BP, the figure of merit, zT, of GeP_5-composited Te sample is significantly improved, as shown in Fig. 7(a) and Fig. S1(f). The zT_{max} of Te + 0.50 wt% GeP_5 sample synthesized at 5.5 GPa is obtained of 0.76 at 524 K, which is ~ 11 times that of the pure Te. In Fig. 7(b), the zT_{ave} presents a progressive increase with the synthetic pressures rising. The peak and average zT values of Te + 0.25 wt% GeP_5 at the temperatures range of 300 K–610 K are increased by 55% and 68% compared with the sample synthesized at 3.0 GPa.

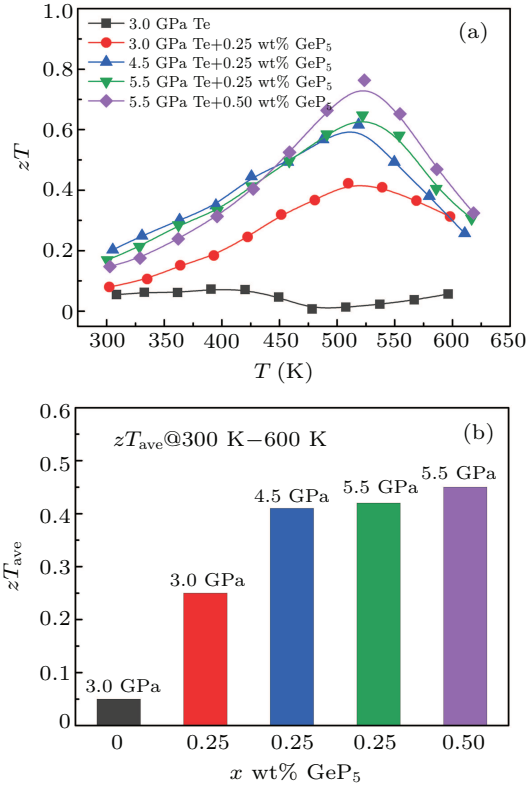


Fig. 7. Temperature-dependent of Te, GeP_5-composited Te samples under different synthetic pressures: (a) figure of merit zT and (b) the average zT value zT_{ave}.

In short, we demonstrated that, under HPHT conditions, the dynamic regulation of carrier behavior and grain boundary density can achieve the double optimization of the electrical property and thermal transport for element Te. The results show that the peak zT of Te + 0.25 wt% GeP_5 synthesized at 5.5 GPa reaches 0.65 at 524 K, which is 55% improvement compared with the lower preparation pressure. Importantly, this work clearly confirms the advantages of pressure that can dramatically modulating the thermoelectric transport properties, being an effective way for searching high performance thermoelectric materials.

Acknowledgements

Project supported by the National Natural Science Foundation of China (Grant Nos. 11804185, 11974208, 52172212, 52102335, and 52002217) and the Natural Science Foundation of Shandong Province, China (Grant Nos. ZR2020YQ05, ZR2019MA054, 2019KJJ020, ZR2021YQ03, and 2022KJA043).

References

[1] Liang Z Q, Chen L D and Bazan G C 2019 *Adv. Electron. Mater.* **5** 1900650
[2] Shi X L, Zou J and Chen Z G 2020 *Chem. Rev.* **120** 7399
[3] Wei T R, Guan M J and Yu J J 2018 *Joule* **2** 2183
[4] Zhao L D, Lo S H and Zhang Y S 2014 *Nature* **508** 373
[5] Kanatzidis M G, Mccarthy T J and Tanzer T A 1996 *ChemInform* **8** 1465

[6] Li Z, Xiao C and Xie Y 2022 *Appl. Phys. Rev.* **9** 011303
[7] Zhai R S, Hu L P and Wu H J 2017 *Appl. Mater. Interfaces* **9** 28577
[8] Chen X, Duan S and Yi W C 2020 *Small* **16** 2001820
[9] Wei Z, Wang C Y and Zhang J Y 2020 *Appl. Mater. Interfaces* **12** 20653
[10] Duan S, Cui Y F and Yi W C 2021 *Appl. Mater. Interfaces* **13** 18800
[11] Lin S Q, Li W and Zhang X Y 2017 *Inorg. Chem. Front.* **4** 1066
[12] Yang M M, Su T C and Zhu H Y 2018 *J. Mater. Sci.* **53** 11524
[13] Duan S, Cui Y F and Chen X 2019 *Adv. Funct. Mater.* **29** 1904346
[14] Lv H Y, Lu W J and Shao D F 2014 *Phys. Rev. B* **90** 085433
[15] Slack G A 1965 *Phys. Rev.* **139** A507
[16] Yang M M, Li X J and Duan S 2022 *Adv. Energy. Mater.* **12** 2203014
[17] Chen X, Duan S and Yi W C 2020 *Small* **16** 2001820
[18] Song J Y, Duan S and Chen X 2020 *Chin. Phys. Lett.* **37** 076203
[19] Duan S, Cui Y F and Yi W C 2022 *Small* **18** 2204197
[20] Guthmann C and Thuillier J M 1970 *Phys. Status. Solidi* **38** 635
[21] Yang H Q, Chen Y J and Wang X Y 2018 *CrystEngComm* **20** 7729
[22] Yang M M, Su T C and Zhou D W 2017 *J. Mater. Sci.* **52** 10526
[23] Lin S Q, Li W and Chen Z W 2016 *Nat. Commun.* **7** 10287
[24] An D C, Chen S P and Zhai X 2020 *J. Mater. Chem. A* **8** 12156
[25] Yang M M, Su T C and Li S S 2021 *J. Alloys Compd.* **887** 161342
[26] Chan T E, Lebeau J M and Venkatasubramanian R 2013 *Appl. Phys. Lett.* **103** 144106
[27] Zhu H Y, Su T C and Li H T 2017 *J. Eur. Ceram. Soc.* **37** 1541
[28] Liu Y X, Wang C and Han S 2021 *Chin. Phys. Lett.* **38** 036201
[29] Chen X, Zhan X H and Wang X J 2021 *Chin. Phys. Lett.* **38** 057402
[30] Adenis C I, Langer V and Lindqvist O 1989 *Acta Cryst.* **C45** 941
[31] Du Y C, Qiu G and Wang Y X 2017 *Nano. Lett.* **17** 3965
[32] Sugai S and Shirotani I 1985 *Solid State Commun.* **53** 753
[33] Fan X, Gao S and Chen Q 2022 *Inorg. Chem.* **61** 8144
[34] Sulaiman S, Izman S and Uday M B 2022 *RSC Adv.* **12** 5428
[35] Pei Y Z, Lalonde A D and Heinz N A 2012 *Adv. Energy. Mater.* **2** 670
[36] Li W, Zheng L L and Ge B H 2017 *Adv. Mater.* **29** 1605887